5A.3

A Practical Delaunay Meshing Algorithm for a Large Class of Domains*

Siu-Wing Cheng[1], Tamal K. Dey[2], and Joshua A. Levine[2]

[1] Dept. of CSE, HKUST, Hong Kong. Email: scheng@cse.ust.hk
[2] Dept. of CSE, Ohio State University, Ohio, USA. Email: tamaldey,levinej@cse.ohio-state.edu

Summary. Recently a Delaunay refinement algorithm has been proposed that can mesh domains as general as piecewise smooth complexes [7]. This class includes polyhedra, smooth and piecewise smooth surfaces, volumes enclosed by them, and above all non-manifolds. In contrast to previous approaches, the algorithm does not impose any restriction on the input angles. Although this algorithm has a provable guarantee about topology, certain steps are too expensive to make it practical.

In this paper we introduce a novel modification of the algorithm to make it implementable in practice. In particular, we replace four tests of the original algorithm with only a single test that is easy to implement. The algorithm has the following guarantees. The output mesh restricted to each manifold element in the complex is a manifold with proper incidence relations. More importantly, with increasing level of refinement which can be controlled by an input parameter, the output mesh becomes homeomorphic to the input while preserving all input features. Implementation results on a disparate array of input domains are presented to corroborate our claims.

1 Introduction

Delaunay refinement is recognized as a versatile tool for meshing geometric domains. Historically, it was developed to mesh polygonal domains in two dimensions [10, 18] and later extended to polyhedral domains in three dimensions [19, 15]. Since the output mesh of a polyhedral domain can conform exactly to the input, topology preservation did not become an issue in these works. For curved domains in two dimensions, topology consideration still remains a mild issue [3]. However, in three dimensions, faithful maintenance of topology becomes a foremost issue. Recently a few works [5, 6, 9] have used Chew's furthest point strategy [11] with the sampling theory [2] to mesh smooth surfaces and volumes enclosed by them [16] with topological guarantees.

*Research supported by NSF, USA (CCF-0430735 and CCF-0635008) and RGC, Hong Kong, China (HKUST 6181/04E).

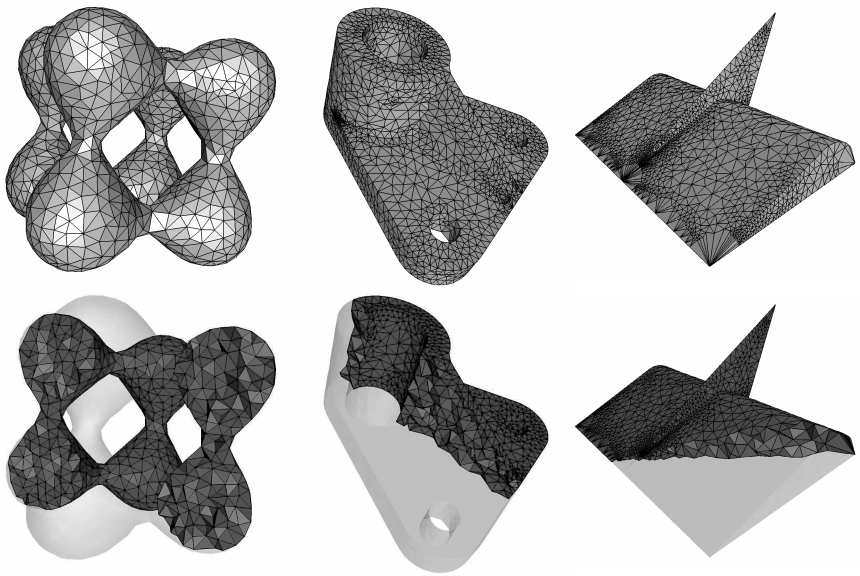

Fig. 1. Meshed PSCs, METABALL (Smooth), PART (Manifold PSC), and WEDGE (Non-manifold, PSC with small angles).

It is well recognized that non-smooth domains pose an added level of difficulty for Delaunay refinement. Boissonnat and Oudot [4] alleviated this problem for a class of surfaces that are only mildly non-smooth as they forbid non-smooth regions subtending small angles. The menace of small angles already appeared in Delaunay meshing of polyhedral domains [9, 17, 20]. Special actions seemed necessary to handle small angles. In a recent work Cheng, Dey, and Ramos [7] succeeded in tackling the problem of non-smoothness with arbitrarily small angles in the input. Drawing upon the idea of protecting small angle regions with balls [9], they protect the curves where different surface patches meet. A novelty of the algorithm is that these protecting balls are turned into weighted points and a Delaunay refinement is run using weighted Delaunay triangulations. The refinement is triggered by violations of some topological conditions introduced by Edelsbrunner and Shah [14] to ensure topology preservations. This algorithm, in theory, enables one to mesh a large class of geometric domains called piecewise smooth complex (PSC). This class includes smooth and non-smooth surfaces both with and without boundaries, volumes enclosed by them, and most importantly non-manifolds. In fact, it is the first algorithm that can compute Delaunay meshes for such a large class of domains with theoretical guarantees. However, the major shortcoming of the algorithm is that it involves expensive computations at each refinement stage making it quite hard for implementation. In this paper we design an algorithm drawing upon the ideas of [7] which is more practical and show its

implementation results on a vast array of disparate domains, see Figure 1 for some examples. Due to space constraints, we skip the proofs of theoretical guarantees which will appear elsewhere.

The original algorithm in [7] inserts points in the domain iteratively after the protection phase with four types of violations, namely (i) a Voronoi edge intersects the domain multiple times, (ii) normals on the curves and surface patches vary beyond a threshold within Voronoi cells, (iii) a Delaunay edge in the restricted triangulation connects vertices across different patches, and (iv) the restricted Delaunay triangles incident to points in a patch do not make a topological disk. We replace these four tests with a single one that only checks for topological disk violations and inserts points in each such case. Once intersections of surface patches with Voronoi edges are determined, this test is purely combinatorial making it easily implementable. Obviously, one cannot hope that the output will have the same topology as the input where refinement is triggered by only this single violation. However, with this 'conservative approach' we are able to guarantee that the output restricted to each stratum of the input is a manifold with vertices on that stratum. Furthermore, if the refinement is carried up to a resolution where the triangles are sufficiently small, the output becomes homeomorphic to the input while preserving the features as well. The main observation is that, in practice, this resolution point is achieved quite fast using a resolution parameter in the algorithm. The protection phase requires some involved computations with curve and surface normals. However, these computations are done only once before the refinement steps. Furthermore, the properties of protecting balls required for the insertion phase to work properly can be satisfied in practice by using sufficiently small balls around the non-smooth edges.

2 Notations and Definitions.

2.1 Domain

Throughout this paper, we assume a generic intersection property that a k-manifold $\sigma \subset \mathbb{R}^3$, $0 \leqslant k \leqslant 3$, and a j-manifold $\sigma' \subset \mathbb{R}^3$, $0 \leqslant j \leqslant 3$, intersect (if at all) in a $(k+j-3)$-manifold if $\sigma \not\subset \sigma'$ and $\sigma' \not\subset \sigma$. We will use both geometric and topological versions of closed balls. A *geometric* closed ball centered at point $x \in \mathbb{R}^3$ with radius $r > 0$, is denoted as $B(x, r)$. We use $\operatorname{int} \mathbb{X}$ and $\operatorname{bd} \mathbb{X}$ to denote the interior and boundary of a topological space $\mathbb{X}$, respectively.

The input domain $\mathcal{D}$ is a piecewise smooth complex (PSC) where each element is a compact smooth (C^2) k-manifold, $0 \leqslant k \leqslant 3$, possibly with boundary. Further, for $0 \leqslant k \leqslant 3$, each element is contained in a smooth k-manifold without boundary. We use $\mathcal{D}_k$ to denote the kth stratum, i.e., the subset of all k-dimensional elements. $\mathcal{D}_0$ is a set of *vertices*; $\mathcal{D}_1$ is a set of

curves called *1-faces*; $\mathcal{D}_2$ is a set of surface patches called *2-faces*; $\mathcal{D}_3$ is a set of volumes called *3-faces*. For $1 \leqslant k \leqslant 2$, we use $\mathcal{D}_{\leqslant k}$ to denote $\mathcal{D}_0 \cup \ldots \cup \mathcal{D}_k$.

The domain $\mathcal{D}$ satisfies the usual proper requirements for being a complex: (i) interiors of the elements are pairwise disjoint and for any $\sigma \in \mathcal{D}$, $\operatorname{bd}\sigma \subset \mathcal{D}$; (ii) for any $\sigma, \sigma' \in \mathcal{D}$, either $\sigma \cap \sigma' = \emptyset$ or $\sigma \cap \sigma'$ is a union of elements in $\mathcal{D}$. We use $|\mathcal{D}|$ to denote the underlying space of $\mathcal{D}$. For $0 \leqslant k \leqslant 3$, we also use $|\mathcal{D}_k|$ to denote the underlying space of $\mathcal{D}_k$.

The definition of $\mathcal{D}$ includes smooth surfaces with or without boundaries, piecewise smooth surfaces including polyhedral surfaces, non-manifold surfaces, and volumes enclosed by them. Figure 1 shows some example inputs that can be handled by our algorithm.

For any point x on a 2-face σ, we use $n_\sigma(x)$ to denote a unit outward normal to the surface of σ at x. For any point x on a 1-face σ, $n_\sigma(x)$ denotes a unit oriented tangent to the curve of σ at x.

2.2 Complexes

Our meshing algorithm generates sample points on the input some of which are weighted. A weighted point p with weight w_p is represented with a ball $\hat{p} = B(p, w_p)$. The squared weighted distance of any point $x \in \mathbb{R}^3$ from $\hat{p}$ is given by $\|x-p\|^2 - w_p^2$. One can define a Voronoi diagram and its dual Delaunay triangulation for a weighted point set just like their Euclidean counterparts by replacing Euclidean distances with weighted distances. For a weighted point set $S \subset \mathbb{R}^3$, let $\operatorname{Vor} S$ and $\operatorname{Del} S$ denote the weighted Voronoi and Delaunay diagrams of S respectively. Each diagram is a cell complex where each k-face is a k-polytope in $\operatorname{Vor} S$ and is a k-simplex in $\operatorname{Del} S$. Each k-face in $\operatorname{Vor} S$ is dual to a $(3-k)$-face in $\operatorname{Del} S$ and vice versa. For a simplex $\xi \in \operatorname{Del} S$ we use V_ξ to denote its dual Voronoi face.

Delaunay refinement for curved domains relies upon restricted Delaunay triangulations [5, 6, 9]. These triangulations consist of Delaunay simplices whose Voronoi duals intersect the domain. We introduce some notations for these structures. Let S be a point set sampled from $|\mathcal{D}|$. For any sub-collection $\mathbb{X} \subset \mathcal{D}$ we define $\operatorname{Del} S|_{\mathbb{X}}$ to be the Delaunay subcomplex restricted to $\mathbb{X}$, i.e., each simplex $\xi \in \operatorname{Del} S|_{\mathbb{X}}$ is the dual of a Voronoi face V_ξ that intersects $\mathbb{X}$ in non-empty set. By above definition, for any $\sigma \in \mathcal{D}$, $\operatorname{Del} S|_\sigma$ denotes the Delaunay subcomplex restricted to the element σ and

$$\operatorname{Del} S|_{\mathcal{D}_i} = \bigcup_{\sigma \in \mathcal{D}_i} \operatorname{Del} S|_\sigma, \qquad \operatorname{Del} S|_{\mathcal{D}} = \bigcup_{\sigma \in \mathcal{D}} \operatorname{Del} S|_\sigma.$$

In case of surfaces restricted Delaunay complexes were considered in previous works because they become topologically equivalent (homeomorphic) when sampled set is sufficiently dense. It turns out that even for PSCs, a similar result holds [7]. However, it is computationally very difficult to determine when the sample is sufficiently dense. To bypass this difficulty we sample the

domain at a resolution specified by the user. We certify that output mesh restricted to each manifold element is a manifold and when the resolution parameter is small enough, it is homeomorphic too. Empirically we observe that homeomorphism is achieved quite early in the refinement process.

The restricted complexes as defined above may contain some superfluous simplices that can be eliminated safely due to a dimensional reason. For example, if the element is a 2-manifold, we can eliminate restricted edges that do not have any restricted triangles incident to it. Similarly, for 1-manifolds, we can eliminate restricted triangles. This motivates defining special sub-complexes of restricted complexes. For $\sigma \in \mathcal{D}_i$, let $\mathrm{Skl}^i\, S|_\sigma$ denote the i-dimensional subcomplex of the restricted Delaunay complex $\mathrm{Del}\, S|_\sigma$, that is,

$$\mathrm{Skl}^i\, S|_\sigma = \mathit{closure}\{t \,|\, t \in \mathrm{Del}\, S|_\sigma \text{ is an } i\text{-simplex}\}.$$

Intuitively, $\mathrm{Skl}^i\, S|_\sigma$ is a i-dimensional complex without any hanging lower dimensional simplices. For example, in Figure 2 the dark edge connecting between upper and lower part of σ is eliminated in $\mathrm{Skl}^2\, S|_\sigma$.

We extend the definition to strata:

$$\mathrm{Skl}^i\, S|_{\mathcal{D}_i} = \bigcup_{\sigma \in \mathcal{D}_i} \mathrm{Skl}^i\, S|_\sigma.$$

Notice that computation of $\mathrm{Skl}^i\, S|_{\mathcal{D}_i}$ is easier than $\mathrm{Del}\, S|_{\mathcal{D}_i}$ since the former one involves computations of intersections only between $(3-i)$-dimensional Voronoi faces with i-faces in $\mathcal{D}$. In fact, because of our special protections of $\mathcal{D}_1$, the only computation we need to determine $\mathrm{Skl}^1\, S|_{\mathcal{D}_1}$ and $\mathrm{Skl}^2\, S|_{\mathcal{D}_2}$ is Voronoi edge-surface intersections.

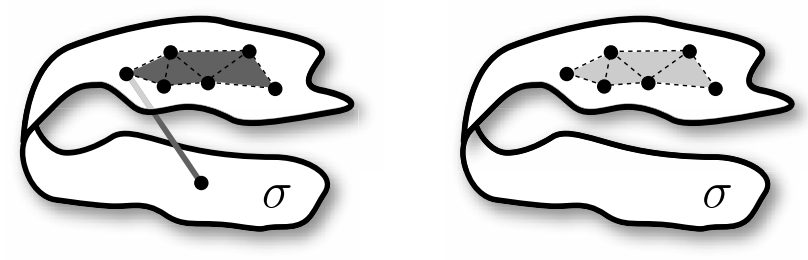

Fig. 2. (left): $\mathrm{Del}\, S|_\sigma$ and (right):$\mathrm{Skl}^i\, S|_\sigma$.

2.3 Overview

As mentioned earlier, Delaunay meshing of PSCs faces difficulty with small input angles that may be subtended at the input curves and vertices. To overcome this difficulty, we protect all elements in $\mathcal{D}_{\leqslant 1}$ with balls that satisfy certain properties. These balls are turned into weighted points for the next stage

of the refinement. Weighted Voronoi diagrams and weighted Delaunay triangulations enter into the picture because of these weighted points. The properties of the protecting balls make sure that the curves in $\mathcal{D}_1$ remain meshed properly throughout the algorithm. In particular, *adjacent* points along any curve in $\mathcal{D}_1$ remain connected with restricted Delaunay edges.

After protection, we insert points iteratively outside the protected regions to mesh 2-faces. This insertion is triggered by a disk condition which essentially imposes that the triangles around a point on a 2-face form a topological disk. After 2-faces are meshed, 3-faces (volumes) are meshed with an usual circumcenter insertion procedure for refining tetrahedra. We show that each inserted point maintains a lower bound on its distances to all existing points. Therefore, the refinement must terminate. At termination the restricted complex $\bigcup_i \mathrm{Skl}^i\, S|_{\mathcal{D}_i}$ is output which has following properties:

Preserved features: All curves in $\mathcal{D}_1$ are meshed homeomorphically with restricted Delaunay edges whose vertices lie on the curves. This preserves non-smooth features or user defined features in the output, see Figure 3.

Faithful topology: All surface patches and volumes in $\mathcal{D}_{\leqslant 3}$ are meshed with a piecewise linear manifold. Furthermore, the algorithm accepts a resolution parameter λ so that it refines the Delaunay triangulations until the restricted triangles have 'size' less than λ. We show that when λ is sufficiently small, the output restricted complex becomes homeomorphic to input $|\mathcal{D}|$.

Fig. 3. Features on ANCHOR are preserved in both surface(middle) and volume(right) meshing.

2.4 Disk conditions

In a mesh of a 2-manifold, the triangles incident to a vertex should form a topological disk. Therefore, one can turn this into a condition for sampling 2-manifolds in the input PSC. Our refinement condition applied to only a single 2-manifold is as simple as this. However, since a PSC may have several 2-manifolds, potentially forming even non-manifolds, one needs to incorporate

some more conditions into the disk condition. Let p be a point on a 2-face σ. Let $\mathrm{Umb}_{\mathcal{D}}(p)$ and $\mathrm{Umb}_{\sigma}(p)$ be the set of triangles in $\mathrm{Skl}^2\, S|_{\mathcal{D}_2}$ and $\mathrm{Skl}^2\, S|_{\sigma}$ respectively which are incident to p. The following disk condition is used for refinement. Once the restricted Delaunay triangles are collected, this check is only combinatorial.

Disk_Conditions(p) : (i) $\mathrm{Umb}_{\mathcal{D}}(p) = \bigcup_{\sigma \ni p} \mathrm{Umb}_{\sigma}(p)$, (ii) for each $\sigma \in \mathcal{D}_2$ containing p, underlying space of $\mathrm{Umb}_{\sigma}(p)$ is a 2-disk which has all vertices in σ. Point p is in the interior of this 2-disk if and only if $p \in \mathrm{int}\,\sigma$. Also, if p is in $\mathrm{bd}\,\sigma$, it is not connected to any other point on $\mathcal{D}_1$ which is not adjacent to it.

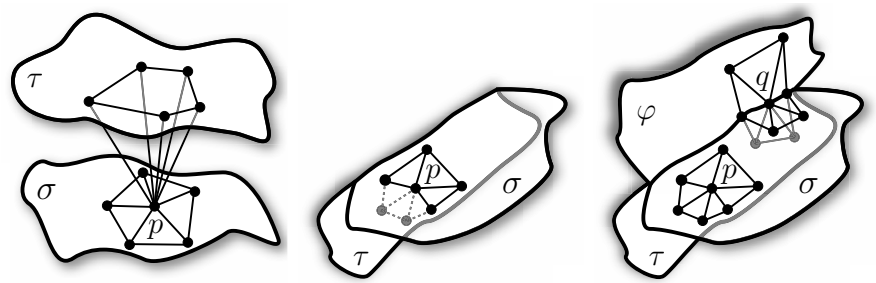

Fig. 4. (left):point $p \in \sigma$ has a disk in σ and another disk in $\tau \neq \sigma$ violating condition (i) (middle): point $p \in \sigma$ has a topological disk but some of its vertices (lightly shaded) belong to τ violating condition (ii), (right): Points p and q satisfy disk condition. Point p, an interior point in σ, lies in the interior of its disk in σ. Point q, a boundary point, has three disks for each of the three 2-faces.

3 Protection

The neighborhoods of the curves and vertices in $\mathcal{D}_{\leqslant 1}$ are regions of potential problems for Delaunay refinements. First, if the elements incident to these curves and vertices make small angles at the points of incidences, usual Delaunay refinement may not terminate. Second, these curves and vertices represent 'features' in the input which should be preserved in the output for many applications. Usual Delaunay refinement may destroy these features [4, 13] or may be made to preserve them for a restricted class of inputs [21]. To overcome these problems we protect elements in $\mathcal{D}_{\leqslant 1}$ with balls and then turn them into weighted points for further meshing following a technique proposed in [7]. The protecting balls should have the following properties.

Protection properties: Let $\omega \leqslant 0.076$ be a positive constant and $\mathcal{B}_p$ denote the protecting ball of a point p.

1. Any two adjacent balls on a 1-face must overlap significantly without containing each other's centers.
2. No three balls have a common intersection.
3. Let $p \in \sigma$ be the center of a protecting ball. Further, let $B = B(p, R)$ be a ball with radius R and center p where $R \leqslant c\,\mathrm{radius}(\mathcal{B}_p)$ for some $c \leqslant 8$.
   (a) For $\tau = \sigma$ or any 2-face incident to σ, $\angle n_\tau(p), n_\tau(z) \leqslant 2\omega$ for any $z \in B \cap \tau$. The same result holds for the surfaces of the 2-faces incident to σ.
   (b) B intersects σ in a single open curve and any 2-face incident to σ in a topological disk. The same result holds for the surfaces of the 2-faces incident to σ.

After computing the protecting balls, we turn each of them into a weighted vertex. That is, for each protecting ball $\mathcal{B}_p$, we obtain the weighted point (p, w_p), where $w_p = \mathrm{radius}(\mathcal{B}_p)$. For technical reasons we need to ensure that each 2-face is intersected by some Voronoi edge in the Voronoi diagram $\mathrm{Vor}\, S$ of the current point set. The weighted vertices ensure it for 2-faces that have boundaries. For 2-faces without boundary, initially we place three weighted points satisfying the protection properties.

After protection, the meshing algorithm inserts points for further Delaunay refinement. These points are not weighted. Also, the refinement step never attempts to insert a point in the interior of any of the protecting balls. In essence, our algorithm maintains a point set S with the following two properties : (i) S contains all weighted points placed in protection step, and (ii) other points in S are unweighted and they lie outside the protecting balls. We call such a point set *admissible*.

The following Lemma proved in [7] is an important consequence of the protection properties.

Lemma 1. *Let S be an admissible point set. Let p and q be adjacent weighted vertices on a 1-face σ. Let σ_{pq} denote the curve segment between p and q. V_{pq} is the only Voronoi facet in* $\mathrm{Vor}\, S$ *that intersects σ_{pq}, and V_{pq} intersects σ_{pq} exactly once.*

4 Meshing PSC

For any triangle $t \in \mathrm{Skl}^2\, S|_\sigma$, define $\mathrm{size}(t, \sigma)$ to be the maximum weighted distance between the vertices of t and points where dual Voronoi edge V_t intersects σ. Notice that if all vertices of t are unweighted, the maximum weighted distance is just the maximum Euclidean distance.

When we mesh volumes, we use the standard technique of inserting circumcenters of tetrahedra that have radius-edge ratio (denoted $\rho()$) greater than a threshold, $\rho_0 \geqslant 1$. If the insertion of the circumcenter threatens to delete any triangle in $\mathrm{Skl}^2\, S|_{\mathcal{D}_2}$, the circumcenter is not inserted. In this case we say that the triangle is encroached by the circumcenter. Essentially, this strategy allows refining most of the tetrahedra except the ones near boundary.

4.1 Algorithm.

The following pseudo-code summarizes our algorithm.

DelPSC $(\mathcal{D}, \lambda, \rho_0)$

1. Protection. Protect elements in $\mathcal{D}_{\leqslant 1}$ with weighted points. Insert three weighted points in each element of $\mathcal{D}_2$ that has no boundary. Let S be the current admissible point set.
2. Mesh2Complex.
   a) Let (p, σ) be any tuple where $p \in S \cap \sigma$ and $\sigma \in \mathcal{D}_2$. If **Disk_Conditions**(p) is violated, find the triangle $t \in \mathrm{Umb}_{\mathcal{D}}(p)$ that maximizes $\mathrm{size}(t, \sigma)$ over all σ containing p and insert $x \in V_t|_\sigma$ that realizes $\mathrm{size}(t, \sigma)$ into S. Go to step 2(c).
   b) If $\mathrm{size}(t, \sigma) > \lambda$ for some tuple (t, σ), where $t \in \mathrm{Skl}^2\, S|_\sigma$, insert $x \in V_t|_{\mathcal{D}}$ that realizes $\mathrm{size}(t, \sigma)$ into S.
   c) Update $\mathrm{Del}\, S$ and $\mathrm{Vor}\, S$.
   d) If S has grown in the last execution of step 2, repeat step 2.
3. Mesh3Complex. For any tuple (t, σ) where t is a tetrahedron in $\mathrm{Skl}^3\, S|_\sigma$
   a) If $\rho(t) > \rho_0$ insert the center of the Delaunay ball (orthoball) of t into S if it does not encroach any triangle in $\mathrm{Skl}^2\, S|_{\mathcal{D}}$.
   b) Update $\mathrm{Del}\, S$ and $\mathrm{Vor}\, S$.
   c) If S has grown in the last execution of step 3, repeat step 3.
4. Return $\bigcup_i \mathrm{Skl}^i\, S|_{\mathcal{D}_i}$.

4.2 Protection computations

To satisfy the protection properties we compute two quantities at the points where balls are centered.

First, we compute the ω-deviation at a point $x \in \sigma$ defined as follows. If $\sigma \in \mathcal{D}_{\leqslant 1}$, for $\omega > 0$, let $\sigma_{x,\omega} = \{y \in \sigma : \angle n_\sigma(x), n_\sigma(y) = \omega\}$. If $\sigma \in \mathcal{D}_2$, define $\sigma_{x,\omega}$ analogously but varying y over the surface of σ. The distance between x and $\sigma_{x,\omega}$ is the ω-deviation radius of x in σ. It is ∞ if $\sigma_{x,\omega} = \emptyset$. Let d_x be the minimum of the ω-deviation radius of x over all σ containing x. By construction, $\angle n_\sigma(x), n_\sigma(y) = \omega$ for some $y \in \sigma$ such that $\|x - y\| = d_x$.

Second, for any 1- or 2-face σ containing x, we compute the tangential contact points between σ and any sphere centered at x. Select the tangential contact point nearest to x (over all 1- and 2-faces containing x). Let d'_x be the distance between x and this nearest tangential contact point.

It is not hard to prove that, for any $r < \min\{d_x, d'_x\}$, $B(x, r) \cap \sigma$ is a closed ball of dimension $\dim(\sigma)$. Also, since $r < d_x$, the normal deviation property 3(a) is satisfied. To satisfy property 1 and 2, we take a fraction of the minimum of d_x and d'_x to determine the size of the ball at x. Let $r_x = \frac{\omega}{8} \min\{d_x, d'_x\}$.

For each curve σ with endpoints, say u and v, we first compute the balls $\mathcal{B}_u$ and $\mathcal{B}_v$ with radii r_u and r_v. Then, starting from, say $\mathcal{B}_u$, we march along

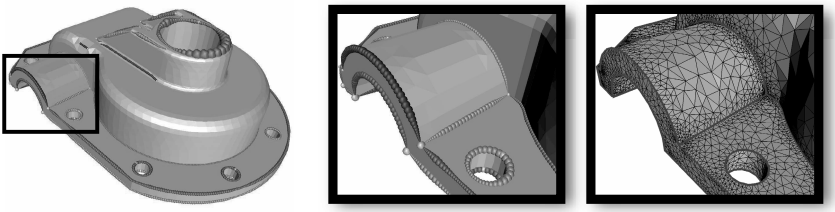

Fig. 5. Protection in action on CASTING. We placed weighted vertices on all elements of $\mathcal{D}_1$ which protect these elements when meshed.

the curve placing the centers of the balls till we reach $\mathcal{B}_v$. These centers can be chosen using a procedure described in [7].

We compute the intersection points $x_0 = \mathcal{B}_v \cap \sigma$ and $x_1 = \mathcal{B}_u \cap \sigma$. The protecting ball at x_1 is $\mathcal{B}_{x_1} = B(x_1, r_{x_1})$. The protecting ball at x_0 is constructed last. We march from $\mathcal{B}_{x_1}$ toward x_0 to construct more protecting balls. For $k \geqslant 2$, let $\mathcal{B}_{x_{k-1}}$ be the last protecting ball placed and let $\mathcal{B}_p$ be the last protecting ball placed before $\mathcal{B}_{x_{k-1}}$. We compute the two intersection points between σ and the boundary of $B(x_{k-1}, \frac{6}{5} r_{x_{k-1}})$. Among these two points let x_k be the point such that $\angle p x_{k-1} x_k > \pi/2$. One can show that x_k is well-defined and x_k lies between x_{k-1} and v along σ. Define

$$r_k = \max \begin{cases} \frac{1}{2}\|x_{k-1} - x_k\| \\ \min_{0 \leqslant j \leqslant k} r_{x_k}/8 + \|x_k - x_j\|/8. \end{cases}$$

If $B(x_k, r_k) \cap B(x_0, r_{x_0}) = \emptyset$, the protecting ball at x_k is

$$\mathcal{B}_{x_k} = B(x_k, r_k).$$

Figure 6 shows an example of the construction of $\mathcal{B}_{x_k}$. We force $r_k \geqslant \frac{1}{2}\|x_{k-1} - x_k\|$ so that $\mathcal{B}_{x_k}$ overlaps significantly with $\mathcal{B}_{x_{k-1}}$. This is desirable because the protecting balls are supposed to cover σ in the end.

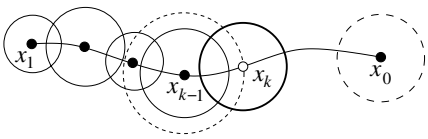

Fig. 6. The two dashed circles denote $B(x_{k-1}, \frac{6}{5} r_{k-1})$ and $B(x_0, r_{x_0})$. The bold circle denotes $\mathcal{B}_{x_k}$.

We continue to march toward x_0 and construct protecting balls until the candidate ball $B(x_m, r_m)$ that we want to put down overlaps with $B(x_0, r_{x_0})$. In this case, we reject x_m and $B(x_m, r_m)$ and compute the intersection points

between σ and the bisector plane of x_{m-1} and x_0. Let y_m be the intersection point that lies between x_{m-1} and x_0 along σ. Finally, the protecting ball at y_m is $\mathcal{B}_{y_m} = B(y_m, R)$ and the protecting ball at x_0 is $\mathcal{B}_{x_0} = B(x_0, R)$, where $R = \frac{2}{3}\|x_{m-1} - y_m\| = \frac{2}{3}\|y_m - x_0\|$. It can be shown that the constructed balls satisfy all protection properties.

Lemma 2. *The protecting balls computed by the above described procedure satisfy the protection properties.*

5 Analysis.

The analysis of DelPSC establishes two main facts: (i) the algorithm terminates, (ii) at termination the output mesh satisfies properties T1-T3 as stated later. It will be essential to prove that DelPSC maintains an admissible point set S throughout its execution.

Lemma 3. DelPSC *never attempts to insert a point in any protecting ball.*

Proof. In Mesh2Complex, points that are intersection of Voronoi edges and $|\mathcal{D}|$ are inserted. Since no three protecting balls intersect, all points on a Voronoi edge have positive distance from all vertices, weighted or not. This means no point of any Voronoi edge lies inside a protecting ball. Therefore, the inserted points in Mesh2Complex must lie outside all protecting balls. For the same reason the orthocenter inserted in Mesh3Complex cannot lie in any of the protecting balls. □

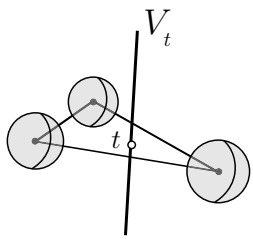

Fig. 7. Inserted points are outside of protecting balls.

5.1 Termination.

We apply the standard argument that there is a lower bound on the distance between each point inserted by DelPSC and all existing points. Then the compactness of $\mathcal{D}$ allows the standard packing argument to claim termination.

The next lemma is the key to proving termination. This result says that if dual Voronoi edges of all restricted triangles incident to a point p in a 2-face σ have nearby intersections with σ, the connected component of σ containing p within V_p satisfies some nice properties. These properties allow one to argue that restricted triangles incident to p will form a disk eventually.

Lemma 4. *Let $p \in S$ be a point on a 2-face σ. Let $\bar{\sigma}$ be the connected component in $V_p|_\sigma$ containing p. There exists a constant $\lambda > 0$ so that following*

holds:

If some edge of V_p *intersects* σ *and* $\mathrm{size}(t, \sigma) < \lambda$ *for each triangle* $t \in \mathrm{Skl}^2 S|_{\mathcal{D}_2}$ *incident to* p*, then*

(i) *there is no 2-face* τ *where* $p \notin \tau$ *and* τ *intersects a Voronoi edge in* V_p*.*
(ii) $\bar{\sigma} = V_p \cap B \cap \sigma$ *where* $B = B(p, 2\lambda)$ *if* p *is unweighted and* $B = B(p, 2\mathrm{radius}(\mathcal{B}_p) + 2\lambda)$ *otherwise;*
(iii) $\bar{\sigma}$ *is a 2-disk;*
(iv) *any edge of* V_p *intersects* $\bar{\sigma}$ *at most once;*
(v) *any facet of* V_p *intersects* $\bar{\sigma}$ *in an empty set or an open curve.*

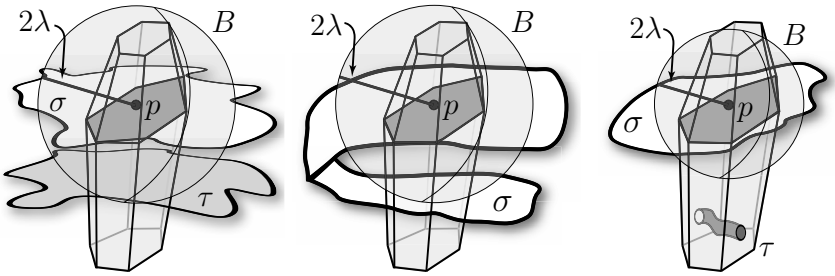

Fig. 8. (left): Within ball B, V_p intersects σ and τ both of which intersect some edge of V_p. This is not possible according to Lemma 4(i), (middle): also not possible since there is another component of σ within $B \cap V_p$ other than $\bar{\sigma}$, (right): Within B, σ intersects V_p in a topological disk. It is possible that there is a different component (τ) which does not intersect any Voronoi edge and hence does not contribute any dual restricted triangle incident to p.

Because of Lemma 4, the restricted triangles incident to a point p on a 2-face σ form a topological disk when λ is sufficiently small (Figure 8). Also, this topological disk cannot include a point from a 2-face other than σ since then the distance between p and that point will be large enough to contradict the resolution level determined by λ.

Theorem 1. DelPSC *terminates.*

Topology Preservation

The output of DelPSC satisfies certain topological properties. Property T1 ensures feature preservation (Figure 9(left)). Property T2 ensures each manifold element is approximated with a manifold and incidence structure among them is preserved (Figure 9(middle)). Property T3 ensures topological equivalence between input and output when resolution parameter is sufficiently small (Figure 9(right) and Figure 10).

(T1) For each $\sigma \in \mathcal{D}_1$, $\mathrm{Skl}^1 S|_\sigma$ is homeomorphic to σ and two vertices are joined by an edge in $\mathrm{Skl}^1 S|_\sigma$ if and only if these two vertices are adjacent on σ.

(T2) For $0 \leqslant i \leqslant 2$ and $\sigma \in \mathcal{D}_i$, $\mathrm{Skl}^i S|_\sigma$ is a i-manifold with vertices only in σ. Further, $\mathrm{bd}\,\mathrm{Skl}^i S|_\sigma = \mathrm{Skl}^{i-1} S|_{\mathrm{bd}\,\sigma}$. For $i = 3$, the statement is true if the set $\mathrm{Skl}^i S|_\sigma$ is not empty at the end of Mesh2Complex.

(T3) There exists a $\lambda > 0$ so that the output mesh of DelPSC($\mathcal{D}$,λ) is homeomorphic to $\mathcal{D}$. Further, this homeomorphism respects stratification with vertex restrictions, that is, for $0 \leqslant i \leqslant 3$, $\mathrm{Skl}^i S|_\sigma$ is homeomorphic to $\sigma \in \mathcal{D}_i$ where $\mathrm{bd}\,\mathrm{Skl}^i S|_\sigma = \mathrm{Skl}^{i-1} S|_{\mathrm{bd}\,\sigma}$ and vertices of $\mathrm{Skl}^i S|_\sigma$ lie in σ.

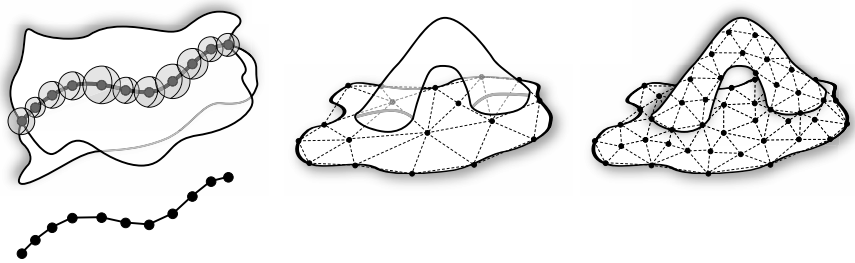

Fig. 9. (left): adjacent points on curves in $\mathcal{D}_1$ are joined by restricted edges, (middle): a surface patch is meshed with a manifold though topology is not fully recovered, (right): topology is fully recovered

The proof of T1 follows immediately from Lemma 1. One requires some nontrivial analysis to prove T2 which we skip here. To prove T3 we need a result of Edelsbrunner and Shah [14].

A CW-complex $\mathcal{R}$ is a collection of closed (topological) balls whose interiors are pairwise disjoint and whose boundaries are union of other closed balls in $\mathcal{R}$. A finite set $S \subset |\mathcal{D}|$ has the extended TBP for $\mathcal{D}$ if there is a CW-complex $\mathcal{R}$ with $|\mathcal{R}| = |\mathcal{D}|$ that satisfies the following conditions for each Voronoi face $F \in \mathrm{Vor}\, S$ intersecting $|\mathcal{D}|$:

(C1) The restricted Voronoi face $F \cap |\mathcal{D}|$ is the underlying space of a CW-complex $\mathcal{R}' \subseteq \mathcal{R}$.
(C2) The closed balls in $\mathcal{R}'$ are incident to a unique closed ball $b_F \in \mathcal{R}'$.
(C3) If b_F is a j-ball, then $b_F \cap \mathrm{bd}\, F$ is a $(j-1)$-sphere.
(C4) Each ℓ-ball in $\mathcal{R}'$, except b_F, intersects $\mathrm{bd}\, F$ in a $(\ell-1)$-ball.

Figure 11 shows two examples of a Voronoi facet F that satisfy the above conditions.

A result of Edelsbrunner and Shah [14] says that if S has the extended TBP for $\mathcal{D}$, the underlying space of $\mathrm{Del}\, S|_{\mathcal{D}}$ is homeomorphic to $|\mathcal{D}|$. Of course, to apply this result we would require a CW-complex with underlying space as

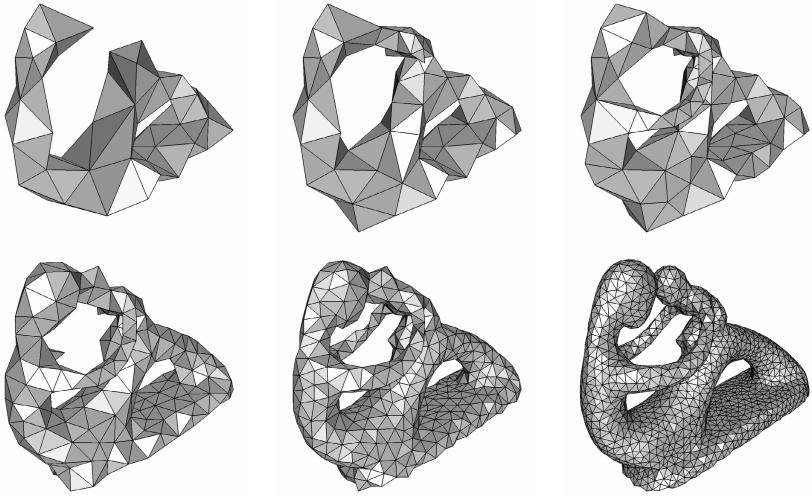

Fig. 10. Output on FERTILITY at different levels of λ. As λ is reduced, eventually the correct topology is achieved.

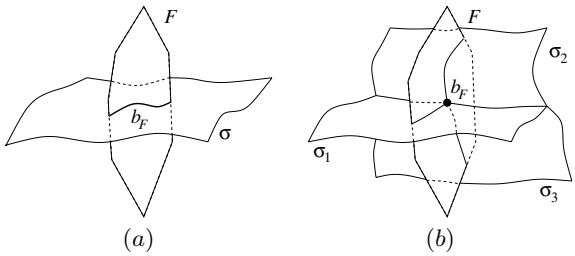

Fig. 11. F is a Voronoi facet. In (a), F intersects a 2-face in a closed topological interval (1-ball) which is b_F. Here b_F intersects $\operatorname{bd} F$ at two points, a 0-sphere. In (b), F intersects the 1-face in a single point which is b_F, and for $1 \leqslant i \leqslant 3$, $F \cap \sigma_i$ are closed topological 1-balls incident to b_F. Here $b_F \cap \operatorname{bd} F = \emptyset$, a -1-sphere.

$|\mathcal{D}|$. We see that when λ is sufficiently small, $\operatorname{Vor} S|_{\mathcal{D}}$ provides such a CW-complex when our algorithm terminates. It can be shown that the following two properties P1, P2 imply Edelsbrunner-Shah conditions C1-C4. Let F be a k-face of $\operatorname{Vor} S$.

(P1) If F intersects an element $\sigma \in \mathcal{D}_j \subseteq \mathcal{D}$, the intersection is a closed $(k+j-3)$-ball.
(P2) There is a unique lowest dimensional element $\sigma_F \in \mathcal{D}$ so that F intersects σ_F and only elements that are incident to σ_F.

One can show that when dual Voronoi edges of all restricted triangles intersect the surface patches within sufficiently small distance from their vertices

(that is, size(t, σ) small), properties P1 and P2 hold. The refinement step 2(b) in DelPSC achieve the required condition when λ is sufficiently small. Also, when P1 and P2 hold, $\mathrm{Del}\, S|_{\mathcal{D}}$ equals $\bigcup_i \mathrm{Skl}^i\, S|_{\mathcal{D}_i}$, the output of DelPSC.

Theorem 2. *The output of* DelPSC *satisfies T1, T2, and T3.*

6 Results

We have implemented the DelPSC algorithm with the aid of the CGAL library for maintaining a weighted Delaunay triangulation. With this implementation we have experimented on a variety of different shapes with varied levels of smoothness, including piecewise-linear (PLC), piecewise-smooth (PSC), and smooth. Our examples incorporate both manifold and non-manifold shapes. Three of these examples also have sharp angles. The different datasets shown in the images are summarized in Table 1. We show the time to mesh each model with the input parameters $\rho_0 = 1.4$ and λ as 10% of the minimum dimension of the bounding box.

Dataset	Smoothness	Manifold	Sharp	Time to Mesh	# of vertices
Serated	PLC	Yes	Yes	94.4 s	13047
Anchor	PSC	Yes	No	43.9 s	7939
Casting	PSC	Yes	No	170.9 s	19810
Part	PSC	Yes	No	22.2 s	3026
Pin-Head	PSC	Yes	Yes	90.1 s	13958
Saturn	PSC	No	No	4.8 s	1340
Swirl	PSC	No	No	86.7 s	9288
Wedge	PSC	No	Yes	9.2 s	2980
Fertility	Smooth	Yes	No	57.7 s	9113
Metaball	Smooth	Yes	No	12.1 s	3288
Hand	Smooth	No	No	24.4 s	4872

Table 1. Datasets.

The input to DelPSC is a polygonal mesh which represents a PSC. We first mark those edges which are non-manifold or have an inner dihedral angle less than a user-specified parameter and then collect them together to form the complex $\mathcal{D}_1$. From $\mathcal{D}_1$ we mark the input polygons into elements of $\mathcal{D}_2$. An octree is built to bucket these input polygons for quick intersection checks with dual Voronoi edges. The next step is to create the protecting balls for elements of $\mathcal{D}_{\leqslant 1}$ as described in section 4. We finally pass all of this information to the Delaunay mesher described as steps 2 and 3.

We show a variety of the output (both surface and volume meshing) for each input models. Figures 12-17 show additional results. In each figure we show the input model, the output surface mesh with the protected elements

highlighted, and the volume mesh output (if it exists). In particular, the FERTILITY and METABALL models (Figures 10 and 1) are taken to be a smooth manifolds, so no input curves are protected. The SWIRL and HAND models (Figures 15 and 17) both have no enclosed volumes, so they do not have a volume mesh associated with them.

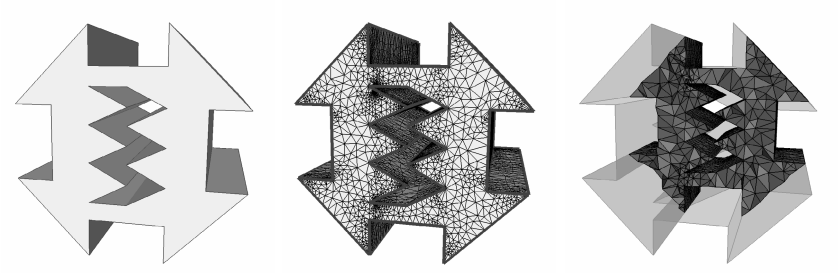

Fig. 12. SERATED: surface (middle) and volume (right) mesh.

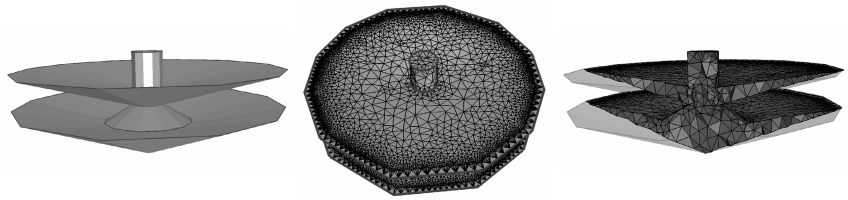

Fig. 13. PIN-HEAD: surface (middle) and volume (right) mesh.

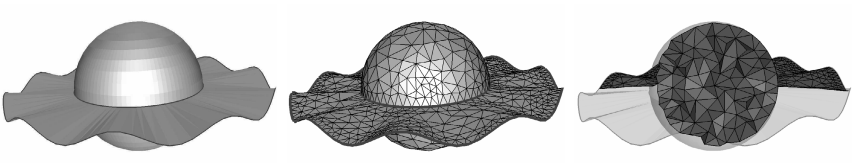

Fig. 14. SATURN: Non-manifold, a surface attached to the equator of a ball.

7 Conclusions

We have presented a practical algorithm to mesh a wide variety of geometric domains with Delaunay refinement technique. The output mesh maintains a manifold property and captures the topology of the input with a sufficient

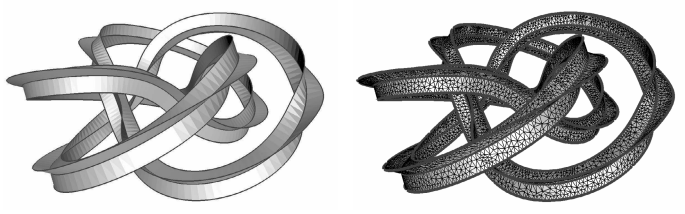

Fig. 15. SWIRL: three surface patches meeting along a curve

Fig. 16. GUIDE: surface (middle) and volume (right) mesh.

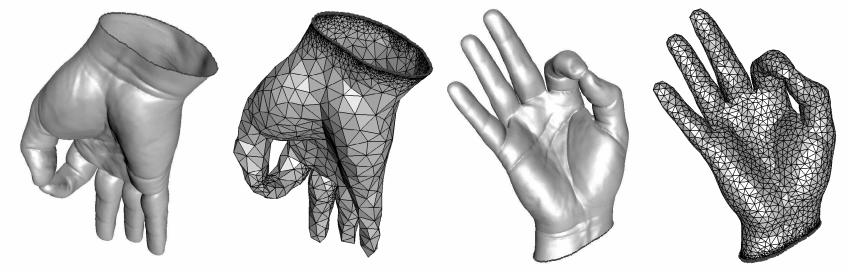

Fig. 17. HAND: manifold with boundary (two levels of refinement).

level of refinement. An interesting aspect of the algorithm is that the input features are preserved in the output.

A number of experimental results validate our claims. It can handle arbitrarily small input angles. When applied to volumes, the algorithm guarantees bounded radius-edge ratio for most of the tetrahedra except near boundary. It can be easily extended to guarantee bounded aspect ratio for most triangles except the ones near non-smooth elements. Furthermore, optimization based techniques can be used to improve qualities of the elements [1].

The question of time and size complexity of the algorithm remains open [12]. Right now the resolution parameter allows uniform refinement. Can it be extended to adaptive refinement? We plan to address these issues in future research.

References

1. P. Alliez, G. Ucelli, C. Goldman, and M. Attene. Recent advances in remeshing of surfaces. State-of-the-art report of AIMSHAPE EU network, 2007.
2. N. Amenta and M. Bern. Surface reconstruction by Voronoi filtering. *Discr. Comput. Geom.*, 22 (1999), 481–504.
3. C. Boivin and C. Ollivier-Gooch. Guaranteed-quality triangular mesh generation for domains with curved boundaries. *Intl. J. Numer. Methods in Engineer.*, 55 (2002), 1185–1213.
4. J.-D. Boissonnat and S. Oudot. Provably good sampling and meshing of Lipschitz surfaces. *Proc. 22nd Ann. Sympos. Comput. Geom.*, 2006, 337–346.
5. J.-D. Boissonnat and S. Oudot. Provably good surface sampling and meshing of surfaces. *Graphical Models*, 67 (2005), 405–451.
6. H.-L. Cheng, T. K. Dey, H. Edelsbrunner, and J. Sullivan. Dynamic skin triangulation. *Discrete Comput. Geom.*, 25 (2001), 525–568.
7. S.-W. Cheng, T. K. Dey, and E. A. Ramos. Delaunay refinement for piecewise smooth complexes. *Proc. 18th Annu. ACM-SIAM Sympos. Discrete Algorithms* (2007), 1096–1105.
8. S.-W. Cheng, T. K. Dey, E. A. Ramos and T. Ray. Quality meshing for polyhedra with small angles. *Internat. J. Comput. Geom. Appl.*, 15 (2005), 421–461.
9. S.-W. Cheng, T. K. Dey, E. A. Ramos and T. Ray. Sampling and meshing a surface with guaranteed topology and geometry. *Proc. 20th Annu. Sympos. Comput. Geom.*, 2004, 280–289.
10. L. P. Chew. Guaranteed-quality triangular meshes. Report TR-98-983, Comput. Sci. Dept., Cornell Univ., Ithaca, New York, 1989.
11. L. P. Chew. Guaranteed-quality mesh generation for curved surfaces. *Proc. 9th Annu. Sympos. Comput. Geom.*, 1993, 274–280.
12. S. Har-Peled and A. Üngör. A time optimal Delaunay refinement algorithm in two dimensions. *Proc. Ann. Sympos. Comput. Geom.*, 2005, 228–236.
13. T. K. Dey, G. Li, and T. Ray. Polygonal surface remeshing with Delaunay refinement. *Proc. 14th Internat. Meshing Roundtable*, 2005, 343–361.
14. H. Edelsbrunner and N. Shah. Triangulating topological spaces. *Internat. J. Comput. Geom. Appl.*, 7 (1997), 365–378.
15. G. L. Miller, D. Talmor, S.-H. Teng and N. Walkington. A Delaunay based numerical method for three dimensions: generation, formulation, and partition. *Proc. 27th Annu. ACM Sympos. Theory Comput.* (1995), 683–692.
16. S. Oudot, L. Rineau, and M. Yvinec. Meshing volumes bounded by smooth surfaces. *Proc. 14th Internat. Meshing Roundtable* (2005), 203–219.
17. S. Pav and N. Walkington. Robust three dimensional Delaunay refinement. *13th Internat. Meshing Roundtable* 2004.
18. J. Ruppert. A Delaunay refinement algorithm for quality 2-dimensional mesh generation. *J. Algorithms*, 18 (1995), 548–585.
19. J. R. Shewchuk. Tetrahedral mesh generation by Delaunay refinement. *Proc. 14th Annu. Sympos. Comput. Geom.* 1998, 86–95.
20. J. R. Shewchuk. Mesh generation for domains with small angles. *Proc. 16th Annu. Sympos. Comput. Geom.*, 2000, 1–10.
21. H. Shi and K. Gärtner. Meshing piecewise linear complexes by constrained Delaunay tetrahedralizations. *Proc. 14th Internat. Meshing Roundtable* (2005), 147–164.